Journal of Experimental Botany, Vol. 58, No. 7, pp. 1903–1913, 2007
doi:10.1093/jxb/erm052 Advance Access publication 18 April, 2007

Journal of Experimental Botany
www.jxb.oxfordjournals.org

RESEARCH PAPER

A model describing cell polyploidization in tissues of growing fruit as related to cessation of cell proliferation

Nadia Bertin[1,*], Alain Lecomte[1], Béatrice Brunel[1], Svetlana Fishman[2] and Michel Génard[1]

[1] *UR1115 Plantes et systèmes de culture horticoles, INRA, F-84000 Avignon, France*

[2] *Department of Statistics and Operations Research, Agricultural Research Organization, The Volcani Center, Bet Dagan 50250, Israel*

Received 21 December 2006; Revised 27 February 2007; Accepted 28 February 2007

Abstract

Endoreduplication is a phenomenon, widespread among plants, which consists of an incomplete cell cycle without mitosis and leads to the increase of the nuclear DNA content. In this work, a model was developed describing cell proliferation and DNA endoreduplication over the whole fruit development, from the pre-anthesis period until maturation. In each mitotic cycle of duration τ, the proportion of cells proceeding through division depends on a constant parameter ρ and on the progressive decline of the proliferating capacity θ. The non-dividing cells may either stop the reduplication fully, or switch to repeated syntheses of DNA without cell division, resulting in cell endoreduplication. A single constant parameter σ describes the proportion of cells that moves from one to the next class of DNA content after each lapse of time τ_E, considered to be the minimum time required for an endocycle. The model calculates the total number of cells and their distribution among eight classes of ploidy level. The dynamic patterns of cell proliferation and ploidy were compared with those obtained experimentally on two contrasting tomato genotypes. The approach developed in this model should allow the future integration of new knowledge concerning the genetic and environmental control of the switch from complete to incomplete cell cycle.

Key words: Cell division, DNA endoreduplication, model, polyploidy, *Solanum lycopersicum*, tomato fruit.

Introduction

Fruit growth starts after bloom with intensive cell division, but, as development proceeds, the proliferative activity of the cells slows down until cell multiplication ceases and the population progressively enters the stage of cell enlargement (Fishman *et al*., 2002; Bertin *et al*., 2003*b*). Cessation of cell division and increase in cell size were found to be closely linked to cell polyploidization (Melaragno *et al*., 1993; Traas *et al*., 1998; Joubès and Chevalier, 2000; Kudo and Kimura, 2002). The increase in nuclear DNA level, concomitant with the arrest of cell multiplication, results from a switch of the complete mitotic cycle to an incomplete cycle called endomitosis (mitotic cycle within the nuclear envelope leading to an increase in the number of chromosomes) or endoreduplication (endonuclear chromosome duplication without sister chromatid segregation leading to an increase in chromosome size) (D'Amato, 1964). A proliferating cell performing a complete cell cycle progresses through the post-mitotic interphase (G_1), replicates its DNA during the synthesis phase (S), grows further during the post-synthetic phase (G_2), and then divides by mitosis (M). Cyclins and cyclin-dependent kinase (CDK) are fundamental regulators of the progression through the different phases of the cell cycle and some of them are specific for the G_1/S or the G_2/M transitions (Francis and Inzé, 2001; Inzé and De Veylder, 2006). Although many factors may be involved, it is admitted that the transition from mitosis to endoreduplication stems from a down-regulation of cyclin-CDK activity at the G_2/M transition, whereas S-phase cyclin-CDK activity is maintained (Grafi and Larkins, 1995; Joubès *et al*., 1999; Edgar and Orr-Weaver, 2001; Inzé and De Veylder, 2006). The switch to endoreduplication has for a long time been considered as irreversible (Matsumara,

* To whom correspondence should be addressed. E-mail: bertin@avignon.inra.fr

2000), but it was recently observed that endoreduplicated cells are able to re-enter mitosis (Weinl *et al*., 2005).

In 90% of angiosperms, endoreduplication is the most common mode of cell polyploidization (Joubès and Chevalier, 2000). According to Nagl (1976), somatic polyploidy occurs in almost all plant species studied so far, resulting in tissues including mixtures of polyploid cells. In maize (*Zea mays* L.) endosperm nuclei with DNA content up to 690C (1C is the DNA content of a haploid nucleus) were measured in some genotypes (Kowles and Phillips, 1985; Larkins *et al*., 2001). In *Arabidopsis thaliana* moderate endoreduplication has been reported in different tissues (up to 32C) (Galbraith *et al*., 1991; Gendreau *et al*., 1998). Lin *et al*. (2001) demonstrated the occurrence of polyploidy in different tissues of orchids (up to 32C). In tomato, large endoreduplicated cells are located in the mesocarp (Bünger-Kibler and Bangerth, 1983) with DNA contents up to 256C or even 512C in cherry tomatoes as well as in large-fruit-size cultivars (Smulders *et al*., 1995; Bergervoet *et al*., 1996; Joubès *et al*., 1999; Bertin *et al*., 2003*a*). In this tissue endoreduplication starts before pollination during the most intensive period of cell division and stops more or less with the cessation of cell expansion (Bertin, 2005).

Many studies describe the endoreduplication dynamic during the development of various species and plant organs or tissues, but the functional role of endoreduplication remains controversial. A lot of works focused on the link between DNA endoreduplication and cell or organ size (Traas *et al*., 1998; Sugimoto-Shirazu and Roberts, 2003). Many authors demonstrated a positive relationship, for instance in epidermis cells of *Arabidopsis* (Melaragno *et al*., 1993); in floral tissues (Kudo and Kimura, 2002; Lee *et al*., 2004); and in root nodules of *Medicago sativa* (Cebolla *et al*., 1999). Among pea seed genotypes, a linear relation was reported between endoreduplication in cotyledon cells and seed dry weight or mean cell volume (Lemontey *et al*., 2000). Similarly, among a large diversity of tomato lines, Cheniclet *et al*. (2005) reported a positive correlation between endoreduplication and the cell size of pericarp tissues. By contrast, the absence of correlation has been reported for mutants affected by the number of endocycles (Leiva-Neto *et al*., 2004), in transgenic lines overexpressing a cell-cycle inhibitor (De Veylder *et al*., 2001), or in response to changes in growth conditions affecting cell size (Bünger-Kibler and Bangerth, 1983; Bertin *et al*., 2003*a*; Bertin, 2005). This controversy highlights complex interactions and compensating effects between the different processes involved, which would be affected differently by many internal and external factors (Cookson *et al*., 2006; Lee *et al*., 2007).

Many theories have been developed to explain the link between cell size and nuclear size or DNA content, such as the nuclear-cytoplasmic ratio theory, but until now the molecular basis of this correlation is poorly understood (Sugimoto-Shirasu and Roberts, 2003). Modelling the dynamic of endoreduplication in various tissues may be useful to understand its regulation and its role in organ growth and sink function. Until now, very few models predict endoreduplication in plant tissue. A functional model of the molecular regulation of the cell cycle has recently been proposed by Beemster *et al*. (2006) to analyse the role of this regulation on cell growth in *Arabidopsis* leaf. This model assumes a first phase of cell proliferation followed by the expansion phase during which endoreduplication occurs. During the proliferation phase, the model states a strong relationship between cell growth and division, as the attainment of a critical ratio between cell size and nuclear DNA content, triggers the expression of different types of cyclins and CDKs regulating the M or S phase. This model succeeds in simulating the effects of an overproduction of cell cycle inhibitor on cell division, cell and leaf expansion of *Arabidopsis*, but endoreduplication was not presented by the authors. A mathematical model based on differential equations, has been proposed by Schweitzer *et al*. (1995) to describe the dynamic of DNA endoreduplication in maize endosperm. This model contains as many parameters as the number of DNA classes, each of them representing the transition rate from one class of C value to the next one. To improve this model, Lee *et al*. (2004, 2007) proposed a sigmoidal decrease of the transition rate over time, determined by two species-dependent parameters. This extended model fits very well with experimental data obtained on orchid flowers with nuclei DNA content up to 16C. It is based on an approach close to that used to describe the dynamics of populations, the total number of cells being an input parameter of the model. In the present study a model of endoreduplication based on the representation of the cell cycle including the transition from the complete to the incomplete cycle is proposed. This model accounts for cell proliferation and ploidization, from the pre-anthesis period until fruit maturation. The objectives of this approach were, first, to make the link between cell division and DNA endoreduplication at the cell and fruit level and, second, to make it possible to integrate, in the future, the fast growing knowledge about the regulation of the mitotic and endoreduplication cycles at the genetic and molecular levels, as done by Beemster *et al*. (2006). The calculated cell number and distribution according to DNA levels during tomato pericarp development was compared with the experimental patterns observed in two contrasting genotypes.

Materials and methods

Plant material

Observations were collected on large-fruited (cv. Levovil) and cherry (cv. Cervil) tomato genotypes of *Solanum lycospersicum*, whose final fresh weight was approximately 150 g and 6 g, respectively. Plants were grown in a greenhouse in the south of

France (Avignon) and sampling took place from April to May. Flower buds and fruits were sampled at different ages related to the time of flower anthesis (full-flower opening), and immediately analysed by flow cytometry. On each inflorescence, half of the fruits were analysed by flow cytometry and the other half were used for the determination of cell number.

Determination of cell number and ploidy level

The number of pericarp cells was measured after tissue dissociation according to a method adapted from that of Bünger-Kibler and Bangerth (1983) and detailed in Bertin *et al*. (2003*b*).

The ploidy was measured in the pericarp tissue after isolation. Either the whole ovary (for small organs before anthesis) or a sample of tissue was chopped out with a razor blade and stained in 2 ml of DAPI solution (4′,6-diamidino-2-phenylindol, PARTEC, GmbH, Germany). Nuclei were filtered through a 30 μm CellTrics® filter, and a sample of 15×10^3 to 20×10^3 nuclei was analysed using a PARTEC flow cytometer (PARTEC Ploidy Analyser PA, GmbH, Germany), equipped with an HBO lamp for UV excitation. The fluorescent signals are presented as frequency distribution histograms. The diploid nuclei of young expanding tomato leaves were used as standard to adjust and check the peak positions within the scale of the histogram. Histograms were analysed with the WinMDI software (version 2.8) to determine the relative number of nuclei containing different amounts of DNA expressed as C values (from 2C to 256C). Three measurements were made in each fruit, when allowed for by its size, and the average value was considered. The mean endoreduplication factor (*EF*) was calculated as proposed by Cookson *et al*. (2006):

$$EF = \sum_{i=1}^{p} \frac{Ci \times p_i}{p_{tot}}$$

where p is the number of peaks of different DNA content (maximum=8) in the sample, C_i is the number of endocycles performed by nuclei in peak i (C_1=0, C_2=1, C_3=2…C_8=7), p_i is the number of nuclei in the peak of value C_i, and p_{tot} is the total number of nuclei in the sample. *EF* indicates the number of endocycles an average cell of the tissue has undergone.

Parameter estimation and statistical estimation of model goodness

A global model was developed to simulate simultaneously the population of proliferating and growing cells with eight ploidy levels from 2C to 256C. To fit this model, a matrix of experimental data including two types of data was built: the first element of the vector represented the total number of pericarp cells and the following elements of the vector indicated the distribution of these cells among the eight DNA-classes. To account for the different nature of data (absolute number of pericarp cell and percentages of cells in each DNA-class), data were weighed by the global variance of the corresponding experimental dataset (cell number or percentage of cells in the different DNA classes).

For the numerical computations of the dynamics of cell population and ploidy level predicted by the model, a computer program based on Matlab language (MathsWork Inc. v.R2006a) was written. The model parameters were estimated with Matlab non-linear procedure, by minimizing the weighed mean squared error (*MSE*) here defined as:

$$MSE = \frac{1}{v_c^2}\sum_{i=1}^{N}\left(y_{cimod} - y_{cidata}\right)^2 + \frac{1}{v_e^2}\sum_{i=1}^{N}\sum_{j=1}^{8}\left(y^j_{eimod} - y^j_{eidata}\right)^2 \quad (1)$$

with y_{imod} being the simulation result and y_{idata} the observed data at date t_i. Indices c and e refer, respectively, to the cell number and endoreduplication data and j refers to the eight classes of DNA content. N is the number of sampling dates, and v_c and v_e are the variances corresponding, respectively, to the cell number and to the percentage of cells in the different DNA classes.

To test the goodness of fit of the model, the root mean squared error (RMSE) (Kobayashi and Us Salam, 2000) was calculated separately for the total cell number and for each level of endoreduplication as:

$$RMSE = \sqrt{\frac{\sum_{i=1}^{N} n_i\left(y_{imod} - \bar{y}_{idata}\right)^2}{\sum_{i=1}^{N} n_i}} \quad (2)$$

with y_{imod} being the simulation result and $\bar{y}_{idata}$ the mean of observed data at date t_i. N is the number of sampling dates, n_i is the sample size at each date t_i. The relative root mean squared error (*RRMSE*) was calculated as the *RMSE* relative to the mean of all observed values. The smaller the *RMSE* or *RRMSE* in comparison to measurements, the better the goodness-of-fit.

The 90% confidence interval of each parameter and the correlations among parameters were calculated using the bootstrap method ('resample' from the original sample with replacement, with the same size as original), considering 200 successive random drawings from the original data set.

Each of the model parameters could be considered as constant or dependent on the fruit development stage. To test for the 'best' model and to decide on the stability of parameters, several alternatives were compared using the maximum likehood criterion of Akaïke. Only the solutions found for the final model will be presented.

Description of the cell proliferation and polyploidization model

General description of the model: The model considers three types of cells: (i) proliferating cells, which participate in the complete mitotic cycles; (ii) non-proliferating cells, which participate in incomplete cycles, and whose nuclei contained different amounts of DNA (C-value from 2 to 256); and (iii) inactive cells, neither dividing, nor endoreduplicating. The proliferating cells divide asynchronously by binary fission, and consequently may be either in 2C (G_1 phase of the cell cycle) or in 4C (G_2 and M phases of the cell cycle) DNA class. The progression of individual dividing cells through the cell cycle was represented in Fig. 1. It was considered that the

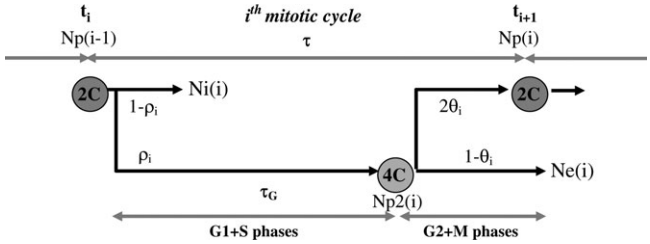

Fig. 1. Scheme of the progression of proliferating cells during the *i*th-mitotic cycle as described in the general model. Np(i), Ni(i), and Ne(i) represent, respectively, the proliferating, inactive, and endoreduplicating cells. $Np_2(i)$ are cells in an intermediate 4C-state between the S (synthesis) and the M (mitosis) phases. ρ_i is the proportion of cells proceeding through division, θ_i is the proliferating activity, τ and τ_G are the durations of the mitotic cycle and G_1+S phases, respectively.

duration τ of one complete cell cycle may be divided into τ_G, corresponding to the duration of the G_1+S phase, and $\tau-\tau_G$ corresponding to the G_2+M phase. A proportion ρ of the proliferating cells proceeds through the cell cycle, whereas the other part, 1–ρ, fully arrests the replication activity and definitely remains in the G_1 phase at 2C state. This type of cells so-called 'inactive' (N_i) are no longer involved in the processes of reduplication considered in this model. After the S phase, a proportion 1–θ exits the cell cycle in the G_2 phase and possibly endoreduplicates (*N*e), whereas the proportion θ performs mitosis and each 4C cell divides in two 2C cells (N_p).

As represented on Fig. 2, a proportion σ_{ijk} of the endoreduplicating cells performs an endocycle entering the 8C DNA class after a time τ_E (minimum duration of an endocycle). In the definition of σ_{ijk}, *i* indicates the mitotic cycle at which cells turned to non-proliferating state, *j* indicates the number of endocycles already performed, and *k* indicates the number of intervals of time τ_E passed from time $t_i+\tau_G$, where $t_i=(i-1)\tau$ is the start time of the *i*th mitotic cycle. The other part, $1-\sigma_{ijk}$, temporarily arrests the reduplication activity, but still has the possibility to endoreduplicate after a given time $k\tau_E$, k being an integer. It was assumed that endoreduplicating and inactive cells could not reenter the mitosis. These processes recur over time, and progressively fill up the successive classes of DNA content.

Kinetics of cell proliferation: In the two following sections, equations are presented which couple the cessation of cell proliferation activity with polyploidization processes. In the model, the cell proliferating activity is given by the proportion ρθ, which is, according to the definition, restricted by intervals $0\leqslant\rho\leqslant1$ and $0\leqslant\theta\leqslant1$. ρ, the proportion of cells entering the division cycle, is considered as constant, whereas θ_i is assumed to decrease after each division event according to a four parameter Fermi function:

$$\theta_i = \frac{(\theta_0-\theta_m)}{1+\exp\left(\frac{t_i-\mu}{a}\right)}+\theta_m \qquad (3)$$

where θ_0 and θ_m indicate the maximum and minimum values of θ_i, μ characterizes the inflection point and *a* indicates the steepness of the decrease in the transition rate from θ_0 to θ_m.

If factors affecting the length of the mitotic cycle, τ, are unchanged during the simulation time, then the time passed after *i* complete cycles is

$$t_{i+1} = i\tau \qquad (4)$$

Let us denote the number of cells at time t_0 as $N(0)=n_0$. During the first cell cycle started at t_0, $\rho\theta_1 n_0$ cells are involved in the division, resulting in $2\rho\theta_1 n_0$ offspring, and $\rho(1-\theta_1)n_0$ cells stop the proliferation to endoreduplicate, whereas ρn_0 cells remain in the S_1 phase and become inactive.

Following the algorithm presented in Fig. 1, the number of proliferating cells which appear after the *i*th mitotic cycle (at time $t=t_{i+1}$) is calculated as

$$Np(t_{i+1}) = 2^i n_0 \prod_{j=1}^{j=i}\theta_j\rho_j \qquad (5)$$

The number of cells which become inactive at the beginning of the *i*th mitotic cycle, is denoted as *Ni*(*i*) and equals to:

$$Ni(i) = (1-\rho_i)Np(t_i) = (1-\rho_i)2^{i-1}n_0\prod_{j=1}^{j=i-1}\theta_j\rho_j \quad {}_j(i\geqslant1) \qquad (6)$$

The number of cells which switch to a non-proliferating, but active state during the *i*th mitotic cycle, i.e. growing cells yet not endoreduplicated, is denoted as *Ne*(*i*) and is equal to:

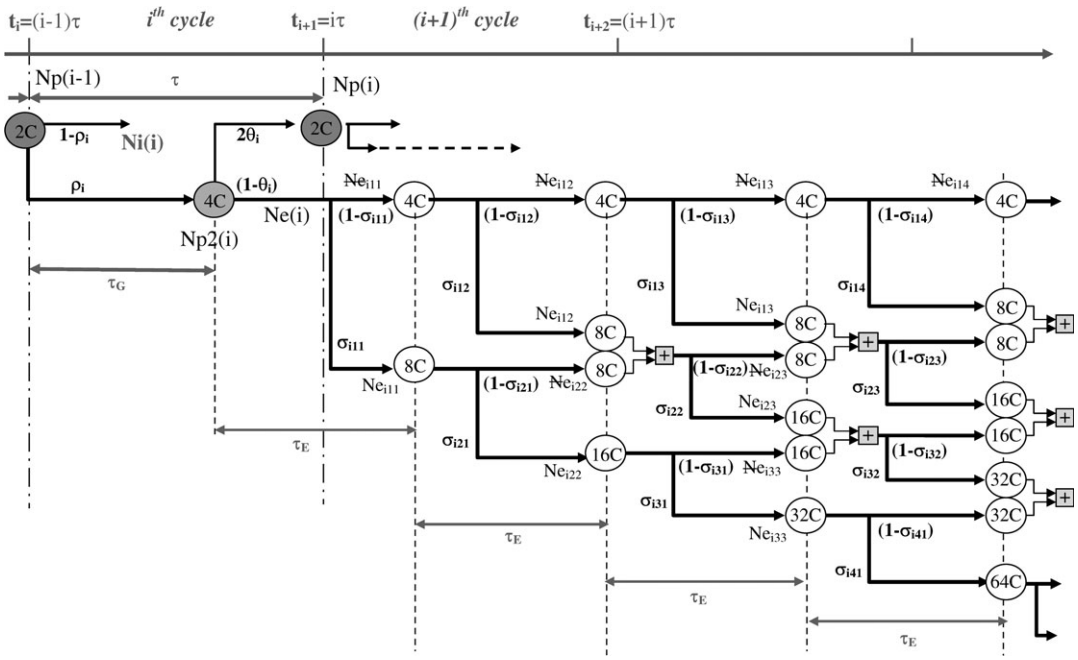

Fig. 2. Global model of cell proliferation and DNA endoreduplication. Closed circles represent complete mitotic cycles, including phases of DNA synthesis, S; mitosis, M; and intermediate G_1 and G_2 phases. Open circles represent successive endocycles performed by cells which escaped the mitotic cycle before the M phase. Np, Ni and Ne indicate, respectively, the proliferating, inactive and endoreduplicating cells. σ_{ijk} is the proportion of cells which performs an endocycle after each lapse of time τ_E, with *i* referring to the *i*th mitotic cycle, *j* to the ploidy increment of the cell and *k* to the number of τ_E intervals of time from the end of the S phase.

$$Ne(i) = (1-\theta_i)\rho_i Np(t_i) = 2^{i-1}(1-\theta_i)n_0 \prod_{j=1}^{j=i-1}\theta_j \prod_{j=1}^{j=i}\rho_j \quad (i \geqslant 1) \tag{7}$$

The total number of inactive cells in the population at time t_{i+1} may be calculated as:

$$Ni(t_{i+1}) = \sum_{m=1}^{m=i} Ni(m) = n_0 \sum_{m=1}^{m=i}(1-\rho_m)2^{m-1}\prod_{j=1}^{j=m-1}\theta_j\rho_j \quad (i \geqslant 1) \tag{8}$$

The total number of growing and active cells in the population at time t_{i+1} may be calculated as:

$$Ne(t_{i+1}) = \sum_{m=1}^{m=i} Ne(m) = n_0 \sum_{m=1}^{m=i}(1-\theta_m)2^{m-1}\prod_{j=1}^{j=m-1}\theta_j\prod_{j=1}^{j=m}\rho_j \quad (i \geqslant 1) \tag{9}$$

The total number of cells in the population at time t_{i+1} is deduced from:

$$N(t_{i+1}) = Np(t_{i+1}) + Ni(t_{i+1}) + Ne(t_{i+1}) \tag{10}$$

Kinetics of polyploidization: Let us consider now what happens to the $Ne(i)$ cells (equation 7) that switched from the proliferating to the non-proliferating state during the ith mitotic cycle. As they exited the mitotic cycle after the S phase, their nuclei DNA content is doubled (4C instead of 2C). The number of 4C-cells appeared after the ith complete cycles is denoted as $\not{Ne}_{i11}=(1-\sigma_{i11})Ne(i)$. The number of cells which immediately perform a round of endoreduplication and got a four times increment of ploidy is denoted as $Ne_{i11}=\sigma_{i11}Ne(i)$. A proportion of these cells further perform some incomplete cycles, each time doubling their DNA content. After j incomplete cycles, the ploidy increment became 2^{j+1}. In the following notation, index k indicates the number of laps of time τ_E passed from time $t_i=(i-1)\tau$. According to the scheme in Fig. 2, the following recurrent equations describe the process:

For $j=1$ and $k=1$

$$Ne_{i11} = \sigma_{i11}\times Ne(i)$$

$$\not{Ne}_{i11} = (1-\sigma_{i11})\times Ne(i)$$

For $j=1$ and $k>1$

$$Ne_{i1k} = \sigma_{i1k}\times \not{Ne}_{i1(k-1)}$$

$$\not{Ne}_{i1k} = (1-\sigma_{i1k})\times \not{Ne}_{i1(k-1)}$$

For $j>1$ and $k=j$

$$Ne_{ijk} = \sigma_{ij(k-j+1)}\times Ne_{i(j-1)(k-1)}$$

$$\not{Ne}_{ijk} = (1-\sigma_{ij(k-j+1)}\times Ne_{i(j-1)(k-1)}$$

For $j>1$ and $k>j$

$$Ne_{ijk} = \sigma_{ij(k-j+1)}\times[Ne_{i(j-1)(k-1)} + \not{Ne}_{ij(k-1)}]$$

$$\not{Ne}_{ijk} = (1-\sigma_{ij(k-j+1)})\times[Ne_{i(j-1)(k-1)} + \not{Ne}_{ij(k-1)}]$$

In the case of $\sigma_{ijk}=cte=\sigma$, the following expressions can be deduced:

$$Ne_{ijk} = C(k-1, j-1)\times\sigma^{j-1}\times(1-\sigma)^{k-j+1}\times Ne(i) \tag{11}$$

$$\not{Ne}_{ijk} = C(k-1, j-1)\times\sigma^{j}\times(1-\sigma)^{k-j}\times Ne(i) \tag{12}$$

with

$$C(n,p) = \frac{n!}{p!\times(n-p)!} \tag{13}$$

Because complete and incomplete cycles are asynchronous, any given instant of time t between t_i and t_{i+1} may be expressed as:

$$t = t_i + \tau_G + k(i)\tau_E = (i-1)\tau + \tau_G + k(i)\tau_E \tag{14}$$

where integer [k(i)] is the number of incomplete cycles potentially performed at time t by the cells that switched to the non-proliferative state during the ith cycle.

At any time, only the cells, which performed i complete cycles during the time t (equation 3), or those which became inactive (equation 5), finished the period with the original ploidy 2C. To account for the asynchronous division in a given tissue, the population of dividing cells was considered as a mixture of 2C and 4C cells, determined by proportions A and (1–A):

$$N_{2C}(t) = A\times Np(t_{i+1}) + \sum_{m=1}^{m=i} Ni(m) \tag{15}$$

The kinetic route of $Ne(i)$ cells is represented by the horizontal and vertical chain in Fig. 2. The total number of cells in 4C-class cumulates the (1–A) proportion of dividing cells and the sum of all $\not{Ne}_{ijk}$:

$$N_{4C}(t) = (1-A)\times Np(t_{i+1}) + \sum_{m=1}^{m=im} \not{Ne}_{mlk(m)} \quad \text{for } j=1 \tag{16}$$

where im is the last complete cell cycle producing non-proliferative cells which get enough time to perform at least one incomplete cycle at time t. Because cells switch to the incomplete cycle in the 4C state, it can be deduced from equation 14 [k(i)=0] that:

$$im = \text{int}\left(\frac{t+\tau-\tau_G}{\tau}\right) \tag{17}$$

More generally, the number of cells in 2^{j+1}C class at time t is given by:

$$N_{2^{j+1}C} = \sum_{m=1}^{m=im} Ne_{m(j-l)k(m)} + \not{Ne}_{mjk(m)} \quad \text{for } k \geqslant j \tag{18}$$

and

$$N_{2^{j+1}C} = \sum_{m=1}^{m=im} Ne_{m(j-l)k(m)} \quad \text{for } k = j-1 \tag{19}$$

with

$$im = \text{int}\left(\frac{t+\tau-\tau_G-(j-1)\tau_E}{\tau}\right) \tag{20}$$

Results and computer simulations

Experimental data are usually presented as percentages of total cell number in the different classes of DNA content, which can be obtained by dividing equations 18 and 19 by equation 10.

Parameterization of the model: The first day of simulation was taken to 8 d before anthesis. At this period no

endoreduplication occurred in the ovary so that all classes of DNA content could be initialized to zero. Assessing the number of cells by enzymatic cell dissociation at this early stage is technically difficult. Few measurements performed on cherry tomatoes (Cervil) allowed estimating n_0 around 0.010×10^6 cells. For large-fruited tomato (Levovil), the initial number was assumed to be around 0.05×10^6, as the ratio of cell number measured at anthesis between Cervil and Levovil was about 5. Although a gradient of cell number within the inflorescence exists for large-fruited genotypes (Bertin *et al.*, 2003*b*), the fruit position was not considered here because no experimental data allowed estimating the difference in initial cell number at 8 d before anthesis.

Considering that the population of proliferating cells in fruit divides asynchronously, it consists of a mixture of 2C and 4C cells at different phases of the mitotic cycle. The proportions of 2C and 4C cells were experimentally found to be constant in dividing organs (floral buds from 20–10 d before anthesis) with 80% of 2C-cells and 20% of 4C-cells (A=0.8 in equations 15 and equations 16). As the fraction of 2C and 4C cells is related to the relative durations of G_1+S and G_2+M phases (Webster and MacLeod, 1980), it was hypothesized that $\tau_G=0.80\tau$. The model was, however, hardly sensitive to the ratio between τ and τ_G.

Parameters θ, ρ, and τ are involved in the dynamic of the proliferating cell population. Parameters σ and τ_E describe the behaviour of cells involved in endocycles. θ is defined by four parameters θ_0, θ_m, μ, and a (equation 3). All other parameters were assumed to be constant under stable growth conditions.

The set of parameters [θ_0, θ_m, μ, a, ρ, τ, τ_E, σ] was then estimated globally by comparing measured observations of total cell number and the proportions of cells with variable nuclear DNA content in the developing tissue of two tomato genotypes, with those calculated by the model. Estimated parameters are given in Table 1 and the dynamic of θ during fruit development is presented in Fig. 3 for both genotypes. The 90% confidence intervals never overlapped except for σ. However, only two parameters strongly differentiated the two genotypes: first, parameter a, i.e. the steepness of the decrease from θ_0 to θ_m (equation 1), was 5–10 times higher in Cervil than in Levovil. Second, τ the duration of one complete cell cycle was twice as high for Levovil (1.93 d) than for Cervil (1 d). Parameter 1–ρ, the proportion of cells that switched to the inactive state during each cell cycle was about 0.03. σ, the proportion of cells that performed a new round of endoreduplication after each lapse of time τ_E was about 1% and τ_E was low around 0.1 d. No clear correlations among parameters could be detected (not shown). For Levovil the strongest correlation was observed between τ and ρ (R=0.74), and for Cervil only θ_m was correlated with θ_0 and μ (R= −0.71 and −0.86, respectively).

Experimental dynamics and model simulation of cell proliferation and ploidy variations in two genotypes

As expected the cell proliferation was quite different between the two genotypes (Fig. 4). From the experimental data, cell division finished 11 d after anthesis (daa) and the final cell number was about 1.17×10^6 cells in the cherry type. In the large-fruited genotype, cell proliferation ceased around 30 daa and reached an average of 10.83×10^6 and 8.36×10^6 cells for the proximal (first to third fruits) and distal (fourth to sixth fruits) positions within the inflorescence, respectively. Fruit maturation occurred more than 15 d earlier for Cervil (around 45 daa) than for Levovil (around 60 daa). The simulated number of pericarp cells fitted well to the experimental data. The shorter duration of the cycle (τ) and the lower proliferation activity (θ) in the pre-anthesis period (from 8 d to 3 d before anthesis) for Cervil (Fig. 3) accounted for the genotype differences. The *RMSE* and *RRMSE* (equation 2) were, respectively, 1.17 and 0.18 for Levovil, and 0.09 and 0.11 for Cervil.

The pattern of endoreduplication, experimentally observed, was similar for large-fruited and cherry tomatoes, except in its timing during fruit development (Fig. 5), and it was independent of the fruit position (not shown). In the young green ovaries, 2C and 4C cells were predominant and during fruit development the tissue became highly polyploid (up to 256C), with a broad distribution of C-values within the pericarp. The increase of 4C cells parallel to the decrease of 2C cells and first appearance of 8C cells, indicated the switch from a state of pure cell

Table 1. *Parameters of the model of cell proliferation and DNA endoreduplication estimated from experimental data of tomato fruit pericarp from cherry (Cervil) and large-fruited (Levovil) genotypes*

The 90% confidence intervals were evaluated by the bootstrap method.

	ρ	μ	a	θ_0	θ_m	τ	τ_E	σ
Levovil	0.974	5.486	1.086	0.977	0.479	1.879	0.127	0.0115
90% confidence intervals	[0.972; 0.992]	[5.175; 5.727]	[0.470; 1.017]	[0.936; 0.980]	[0.474; 0.489]	[1.856; 2.065]	[0.108; 0.126]	[0.0099; 0.0134]
Cervil	0.965	5.943	5.046	0.894	0.431	1.00	0.098	0.0094
90% confidence intervals	[0.962; 0.971]	[5.827; 6.579]	[4.392; 5.776]	[0.875; 0.910]	[0.401; 0.442]	[0.958; 1.088]	[0.089; 0.100]	[0.0083; 0.0100

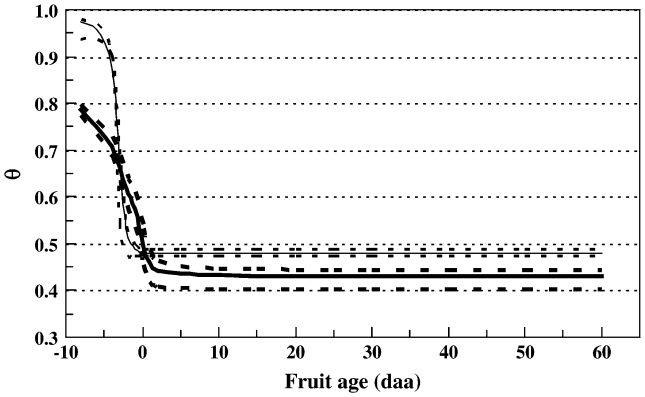

Fig. 3. Dynamic of the proliferative activity θ estimated for cherry (Cervil: bold line) and large-fruited (Levovil: thin line) tomato genotypes. Broken lines represent the 90% confidence intervals of the parameter estimated by the bootstrap method.

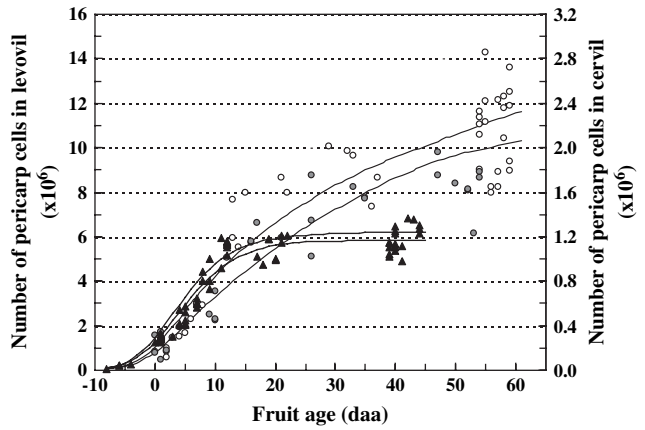

Fig. 4. Comparison of experimental data and simulated number of pericarp cells in cherry (Cervil: triangles and bold lines) and large-fruited (Levovil: circles and thin lines) tomatoes. For Levovil, open and closed symbols represent proximal and distal fruit positions. Dots are the measured cell number for individual fruits. Lines are model simulations with upper and lower limits of 90% confidence intervals of parameter values given in Table 1.

proliferation to a state of concomitant proliferation and endoreduplication. This occurred around 9–10 d and 5–6 d before anthesis in Cervil and Levovil, respectively (data not shown). As endoreduplication started latter in Levovil than in Cervil, the emergence of the successive C-classes was also delayed, except for the 128C and 256C classes (Fig. 5). Globally, the simulated timing and dynamics of the eight DNA classes fitted well to the experimental observations. The lower value of θ_0 and τ_E for cherry tomato mainly accounted for the genetic differences of timing during fruit development. However, these differences were overestimated by the model for the last two C-classes (128C and 256C) since the experimental data were similar for the two genotypes. The 256C class was largely overestimated by the model for both genotypes, but this class represents only a small percentage of cells and the peak detection may not be accurate. The *RMSE* (given in Fig. 5 legends) ranged from 1.14 (256C) to 6.96 (4C) for Levovil, and from 1.94 (128C) to 6.94 (4C) for Cervil.

The mean endoreduplication factor (*EF*) calculated from measurements increased faster during the preanthesis period in Cervil than in Levovil, but a similar value of 3.5 endocycles was achieved at maturity in both genotypes due to the longer period of development for Levovil (Fig. 6). *EF* was well predicted by the model.

Discussion

A mechanistic model of cell multiplication and DNA endoreduplication is presented here, which describes the phenomenological development of (i) mitotic cycles, (ii) transition from mitotic cycle to endoreduplication cycle, and (iii) further endoreduplication rounds, each process involving specific parameters. The switch from mitotic cycle to endocycle is described in an integrative manner through parameter θ, whereas the progress through the successive rounds of endoreduplication is controlled by σ and τ_E. Parameterization of this model was made on the basis of experimental data from tomato pericarp, a tissue highly polyploid and thus especially interesting to evaluate the model. The patterns of ploidy variations observed in this study agreed with the literature (Bergervoet *et al*., 1996; Joubès and Chevalier, 2000; Bertin *et al*., 2003*a*, 2005; Cheniclet *et al*., 2005) and the mean ploidy obtained here for the two genotypes roughly corresponded to the mean value reported by Cheniclet *et al*. (2005) for 20 different tomato genotypes. Interestingly, the final mean number of endocycles was similar in cherry and large-fruited tomatoes due to different timing of endoreduplication and different periods of development, rather than to different rate of endoreduplication. This suggests that the switch from the mitotic cycle to the endocycle and the duration of the development period were the main factors involved in genetic differences between these two genotypes, whereas the process of endoreduplication itself would be similarly regulated. The fact that similar numbers of endocycles were performed in both genotypes (Fig. 6) indicates that endoreduplication was not the reason for the difference in cell size, about 3–4 times smaller in Cervil (data not shown). It rather supports the hypothesis that the final amount of DNA was developmentally programmed.

The progression through the cell cycle is regulated by various CDKs, whose activity is temporarily regulated (Grafi, 1998). The control of the switch from complete cycle to incomplete cycle is probably the most crucial point controlling the balance between cell proliferation and cell differentiation. Many examples in the literature illustrate the fact that a down- or up-regulation of the mitotic activity often has some opposite effects on endoreduplication. For instance, a down-regulation of mitotic inhibitor decreases mean endoreduplication and

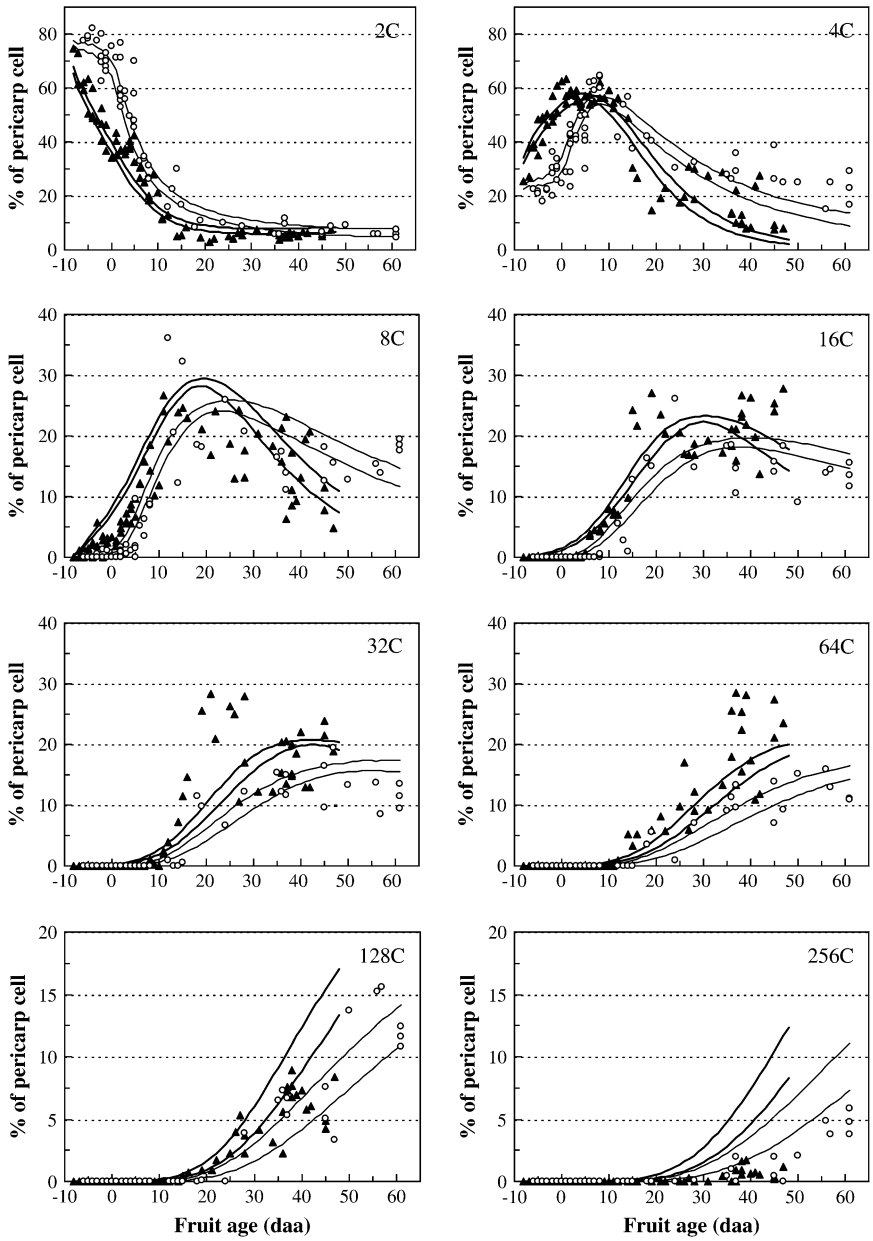

Fig. 5. Comparison of experimental data and fitted curves of the distribution of pericarp cells among classes of nuclear DNA content for cherry (Cervil: triangles and bold lines) and large-fruited (Levovil: circles and thin lines) tomato genotypes. Dots are the measured ratio of cell number (NiC/N) at 2C (A), 4C (B), 16C (C), 32C (D), 64C (E), 128C (E), and 256C (F). Lines are model simulations with upper and lower limits of 90% confidence intervals of parameter values given in Table 1. Root mean squared errors (RMSE) for the eight successive classes are 4.46, 6.96, 4.51, 3.10, 2.47, 1.75, 1.56, and 1.14 for Levovil and 4.02, 6.94, 4.69, 3.56, 4.95, 3.73, 1.94, and 2.29 for Cervil.

leads to smaller cell size (Cebolla *et al.*, 1999). The control of the G2/M transition probably drives the mitotic cycle/endocycle transition, involving inhibitors of specific regulators of the M phase (Joubès *et al.*, 1999; Larkins *et al.*, 2001; Bisbis *et al.*, 2006) designated as Mitosis-Inducing Factors (MIF) by Inzé and De Veylder (2006). Although the endocycle is not only a truncated mitotic cycle and may require additional factors than those involved in the S phase of the mitotic cycle (Sugimoto-Shirasu and Roberts, 2003), it was proposed that 'the difference between the mitotic cycle and the endocycle must be locked for in the mechanism regulating G_2-to-M transition' (Inzé and De Veylder, 2006). This was represented in the model as an exit from the G_2 phase of the mitotic cycle, hypothetically due to the inhibition or down-regulation of MIF.

Grafi (1998) identified three types of endoreduplication: (i) type I in which multiple initiations of DNA synthesis occur within a given S phase; (ii) type II consisting of re-occurring S phases; and (iii) type III consisting of repeated

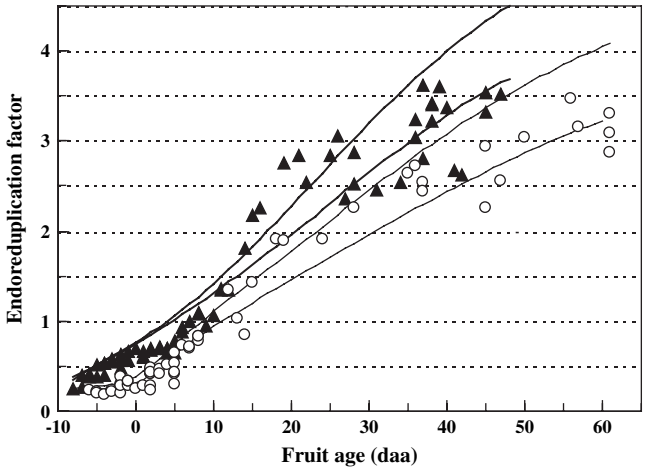

Fig. 6. Comparison of experimental data and fitted curves of mean endoreduplication factor for cherry (Cervil: triangles and bold lines) and large-fruited (Levovil: circles and thin lines) tomato genotypes. Lines are model simulations with upper and lower limits of 90% confidence intervals of parameter values given in Table 1.

S and Gap phases. In Fig. 3, type I and II are designed by the σ_{ijk} proportions of cells which underwent multiple rounds of endoreduplication without gap phases, whereas type III is represented by $(1-\sigma_{ijk})$ proportions of cells, for which one or more gap phases may occur before the initiation of the next S phase. τ_E is the time during which a certain proportion of non-proliferative cell had enough time to endoreduplicate, and logically it was found to be short (0.10 and 0.13 d for Cervil and Levovil, respectively). Since it represents the minimum time needed for a cell to endoreduplicate corresponding to type II defined by Grafi (1998), τ_E may be roughly assimilated with the duration of the S phase.

According to the model, the genetic differences were mainly ascribed to two parameters: τ the duration of the cell cycle and θ_0 the initial proportion of cells that proceeds through division during the first cycle, both lower for Cervil than for Levovil. The lower value of θ_0 mainly resulted from the fact that Cervil fruits were physiologically older at the initial time (8 d before anthesis) than Levovil fruits, as outlined by the earlier (about 4 d) onset of endoreduplication in Cervil. The duration of one complete cell cycle was 1.00 d and 1.88 d for Cervil and Levovil, respectively. The estimated value of τ is largely influenced by the initial number of cells. Initialization of simulated variables is always tricky in modelling, and this is worsened here as measuring the number of cells in young floral organs is technically difficult. New methods should be developed to assess these data precisely. In a previous work focusing on the modelling of cell proliferation, a value of 2.6 d was found for τ for a beef tomato cultivar (Bertin *et al.*, 2003*b*). Rare experimental data are available for tomato fruit in the literature. Cell-cycle durations reported for other species are 1.3–1.7 d for sunflower leaves (Granier and Tardieu, 1998), 18 h for *Arabidopsis* root (Beemster and Baskin, 1998), 20 h for *Arabidopsis* leaf (De Veylder *et al.*, 2001) or 5.4–0.45 d for root meristems of *Allium cepa* as the temperature rose from 5 °C to 35°C (López-Sáez *et al.*, 1966). The environmental and genetic influence on this parameter should be considered in the future. Yang *et al.* (2006) suggested that the cell cycle consists of two phases: a variable period called sizer-phase, which is the required time for a cell to reach the critical size to divide, and a constant period called timer-phase mainly independent of size. Such a concept may be applied to account for genetic (timer-phase) and environmental (sizer-phase) controls of τ.

Before endoreduplication starts, around 5–10 d before anthesis according to the genotype, the ovary exclusively contains 2C and 4C cells, accounting for about 80% and 20% of total cells, respectively. These values (20–80%) are quite close to those observed on cabbage petals (Kudo and Kimura, 2002) or in orchid flowers (Lee *et al.*, 2004). The persistence of 2C cells at the mature green and the ripe stage has been reported in tomato by many authors (Bergervoet *et al.*, 1996; Joubès and Chevalier, 2000; Bertin, 2003*a*, 2005), in contrast to Cheniclet *et al.* (2005). The presence of 2C cells indicated that they did not or stopped participate in the endoreduplication process, otherwise they would be rapidly exhausted. In the present model, parameter ρ accounts for these cells, which are assumed to exit the mitotic cycle in the G_1 phase.

After parameterization, the model was able to simulate accurately the number of cells, their distribution among the ploidy levels and the mean *EF*. The bad estimations of the last classes may be partly due to the low number of cells in these classes, often close to the detection limit of the flow cytometer. However, other hypotheses may be put forward. The gap between simulated and measured data occurred more or less when cell or fruit expansion ceased (data not shown), which occurred earlier in Cervil than in Levovil. These results suggested that endoreduplication was down-regulated during fruit development. In their model, Lee *et al.* (2004) considered that the transition rate of cells from one DNA class to the next is described by a Fermi function of time, the initial rate decreasing with the DNA content. This assumes that the ability to perform another round of endoreduplication decreases as the nuclei DNA content grows up. In the present study, parameter σ_{ijk} is crucial for the fluxes of cells among the DNA-classes. It may depend on *i* the cycle number related to fruit ageing; on *k* the number of laps of time τ_E passed since the cell became non-proliferative; or on *j* the number of endoreduplication rounds already performed by the cell. The decrease of σ might be related to: (i) a longer S phase stemmed from the increasing nucleus size; (ii) the down-regulation of specific S phase CDKs; and/or (iii) the occurrence of inhibitors of the S phase CDKs during fruit development. No biological information settles this

question clearly. It is suggested that σ would be constant during the period of cell division and expansion of tomato pericarp, and that it would steeply decrease as cell expansion ceases. The seventh and eighth round of endoreduplication occurring during the phase of maturation, other metabolic controls may be involved, for instance the emission of ethylene (Gendreau *et al*., 1999; Dan *et al*., 2003). More knowledge is necessary to understand the control of endoreduplication during fruit maturation and to propose a function for σ.

Conclusion and perspectives

The model developed in this study attempted to describe the link between mitotic cycle and endocycle at fruit scale from the preanthesis period until maturation. For this purpose, a relatively high number of parameters was required, but each of them has a physiological significance and seems to be essential. One perspective is to link this model with a model of cell expansion, which is supposed to determine the hierarchical relationships between cell growth and proliferation and between cell growth and endoreduplication, for instance, as suggested by Beemster *et al*. (2006). This may be done in the frame of the virtual fruit proposed by Génard *et al*. (2007) and it would probably generate new insight into the debated role of endoreduplication in the regulation of cell/fruit growth. The model also addresses new questions for biologists through the functions and dynamics of its parameters and it may be used to perform virtual experiments very easily and at very low cost. As ecophysiological simulation models describe interactions and feedback regulations among the fruit system components, they may generate unexpected properties, so-called emergent properties (Génard *et al*., 2007). In the present model, this may be simply achieved by analysing the effects of changing one factor or one parameter on the output or intermediate variables. For instance, let it be assumed that the rate of decrease in θ reflects the decreasing amount or down-regulation of MIF activity by increasing the amount of specific inhibitors. Then changing the dynamics of θ without changing any other parameter may help to predict how, in diverse conditions, the molecular control of the G_2/M transition may affect the balance between proliferation and endoreduplication during fruit development. Confronting model simulations and parameters with a molecular analysis of the main MIF inhibitors may help to determine the importance of the numerous controlling factors involved in the onset of endoreduplication. However, for this purpose a first step will be to include in the model the main internal and environmental controls of its parameters, for instance, by sugars and hormones (Bohner and Bangerth, 1988; Joubès and Chevalier, 2000; Baldet *et al*., 2006), light (Gendreau *et al*., 1998), temperature (Bertin, 2005; Lee *et al*., 2007), or soil water content (Cookson *et al*., 2006). This will be the matter of future investigations.

References

Baldet P, Hernould M, Laporte F, Mounet F, Just D, Mouras A, Chevalier C, Rothan C. 2006. The expression of cell proliferation-related genes in early developing flowers is affected by a fruit load reduction in tomato plants. *Journal of Experimental Botany* **57,** 961–970.

Beemster GTS, Baskin TI. 1998. Analysis of cell division and elongation underlying the developmental acceleration of root growth in *Arabidopsis thaliana*. *Plant Physiology* **116,** 515–526.

Beemster GTS, Vercruysse S, De Veylder L, Kuiper M, Inzé D. 2006. The *Arabidopsis* leaf as a model system for investigating the role of cell cycle regulation in organ growth. *Journal of Plant Research* **119,** 43–50.

Bergervoet JHW, Verhoeven HA, Gilissen LJW, Bino RJ. 1996. High amounts of nuclear DNA in tomato (*Lycopersicon esculentum* Mill.) pericarp. *Plant Science* **116,** 141–145.

Bertin N. 2005. Analysis of the tomato fruit growth response to temperature and plant fruit load in relation to cell division, cell expansion, and DNA endoreduplication. *Annals of Botany* **95,** 439–447.

Bertin N, Borel C, Brunel B, Cheniclet C, Causse M. 2003*a*. Do genetic makeup and growth manipulation affect tomato fruit size by cell number, or cell size and DNA endoreduplication? *Annals of Botany* **92,** 415–424.

Bertin N, Fishman S, Génard M. 2003*b*. A model for early stage of tomato fruit development: cell multiplication and cessation of the cell proliferative activity. *Annals of Botany* **92,** 65–72.

Bisbis B, Delmas F, Joubès J, Sicard A, Hernould M, Inzé D, Mouras A, Chevalier C. 2006. Cyclin-dependent kinase (CDK) inhibitors regulate the CDK-cyclin complex activities in endoreduplication cells of developing tomato fruit. *Journal of Biological Chemistry* **281,** 7373–7383.

Bohner J, Bangerth F. 1988. Effects of fruit set sequence and defoliation on cell number, cell size and hormone levels of tomato fruits (*Lycopersicon esculentum* Mill.) within a truss. *Plant Growth Regulation* **7,** 141–155.

Bünger-Kibler S, Bangerth F. 1983. Relationship between cell number, cell size and fruit size of seeded fruits of tomato (*Lycopersicon esculentum* Mill.), and those induced parthenocarpically by the application of plant growth regulators. *Plant Growth Regulation* **1,** 143–154.

Cebolla A, Vinardell JM, Kiss E, Olah B, Roudier F, Kondorosi A, Kondorosi E. 1999. The mitotic inhibitor ccs52 is required for endoreduplication and ploidy-dependent cell enlargement in plants. *EMBO Journal* **18,** 4476–4484.

Cheniclet C, Rong WY, Causse M, Frangne N, Bolling L, Carde JP, Renaudin JP. 2005. Cell expansion and endoreduplication show a large genetic variability in pericarp and contribute strongly to tomato fruit growth. *Plant Physiology* **139,** 1–11.

Cookson SJ, Radziejwoski A, Granier C. 2006. Cell and leaf size plasticity in Arabidopsis: what is the role of endoreduplication? *Plant, Cell and Environment* **29,** 1273–1283.

D'Amato F. 1964. Endopolyploidy as a factor in plant tissue development. *Caryologia* **17,** 41–52.

Dan H, Imaseki H, Wasteneys GO, Kazama H. 2003. Ethylene stimulates endoreduplication but inhibits cytokinesis in cucumber hypocotyls epidermis. *Plant Physiology* **133,** 1726–1731.

De Veylder L, Beeckman T, Beemster GTS, Krols L, Terras F, Landrieu I, Van Der Schueren E, Maes S, Naudts M, Inzé D.

2001. Functional analysis of cyclin-dependent kinase inhibitors of *Arabidopsis*. *The Plant Cell* **13,** 1653–1668.

Edgar BA, Orr-Weaver TL. 2001. Endoreduplication cell cycles: more or less. *Cell* **105,** 297–306.

Fishman S, Bertin N, Génard M. 2002. Cell division and cessation of cell proliferation in growing fruit. *Acta Horticulturae* **584,** 125–131.

Francis D, Inzé D. 2001. The plant cell cycle. In: Francis D, ed. *The plant cell cycle and its interfaces*. UK: Academic Press, 1–18.

Galbraith DW, Harkins KR, Knapp S. 1991. Systematic endopolyploidy in *Arabidopsis thaliana*. *Plant Physiology* **96,** 985–989.

Génard M, Bertin N, Borel C, *et al*. 2007. Towards a virtual fruit focusing on quality: modelling features and potential uses. *Journal of Experimental Botany*. (in press).

Gendreau E, Höfte H, Grandjean O, Broun S, Traas J. 1998. Phytochrome controls the number of endoreduplication cycles in the *Arabidopsis thaliana* hypocotyl. *The Plant Journal* **13,** 221–230.

Gendreau E, Höfte H, Orbovic V, Traas J. 1999. Gibberellin and ethylene control endoreduplication levels in the *Arabidopsis thaliana* hypocotyls. *Planta* **209,** 513–516.

Grafi G. 1998. Cell cycle regulation of DNA replication: the endoreduplication perspective. *Experimental Cell Research* **244,** 372–378.

Grafi G, Larkins BA. 1995. Endoreduplication in maize endosperm: involvement of M phase-promoting factor inhibition and induction of S phase-related protein kinases. *Science* **269,** 1262–1264.

Granier C, Tardieu F. 1998. Spatial and temporal analyses of expansion and cell cycle in sunflower leaves. *Plant Physiology* **116,** 991–1001.

Inzé D, De Veylder L. 2006. Cell-cycle regulation in plant development. *Annual Review of Genetics* **40,** 77–107.

Joubès J, Chevalier C. 2000. Endoreduplication in higher plants. *Plant Molecular Biology* **43,** 735–745.

Joubès J, Phan T-H, Just D, Rothan C, Bergounioux C, Raymond P, Chevalier C. 1999. Molecular and biochemical characterization of the involvement of cyclin-dependent kinase A during the early development of tomato fruit. *Plant Physiology* **121,** 857–869.

Kobayashi K, Us Salam M. 2000. Comparing simulated and measured values using mean squared deviation and its component. *Agronomy Journal* **92,** 345–352.

Kowles RV, Phillips RL. 1985. DNA amplification patterns in maize endosperm nuclei during kernel development. *Proceedings of the National Academy of Sciences, USA* **82,** 7010–7014.

Kudo N, Kimura Y. 2002. Nuclear DNA endoreduplication during petal development in cabbage: relationship between ploidy levels and cell size. *Journal of Experimental Botany* **53,** 1017–1023.

Larkins BA, Dilkes BP, Dante RA, Coelho CM. 2001. Investigating the hows and whys of DNA endoreduplication. *Journal of Experimental Botany* **52,** 183–192.

Lee H-C, Chen Y-J, Markhart AH, Lin T-Y. 2007. Temperature effects on systemic endoreduplication in orchid during floral development. *Plant Science* **172,** 588–595.

Lee H-C, Chiou D-W, Chen W-H, Markhart AH, Chen Y-H, Lin T-Y. 2004. Dynamics of cell growth and endoreduplication during orchid flower development. *Plant Science* **166,** 659–667.

Leiva-Neto JT, Grafi G, Sabelli PA, Woo YM, Dante RA, Maddock S, Gordon-Kamm WJ, Larkins BA. 2004. A dominant negative mutant of cyclin-dependent kinase A reduces endoreduplication but not cell size or gene expression in maize endosperm. *The Plant Cell* **16,** 1854–1869.

Lemontey C, Mousset-De'clas C, Munier-Jolain N, Boutin P. 2000. Maternal genotype influences pea seed size by controlling both mitotic activity during early embryogenesis and final endoreduplication level/cotyledon cell size in mature seed. *Journal of Experimental Botany* **51,** 167–175.

Lin S, Lee H-C, Chen W-H, Chen C-C, Kao Y-Y, Fu Y-M, Chen Y-H, Lin T-Y. 2001. Nuclear DNA contents of *Phalaenopsis* sp. and *Doritis pulcherrima*. *Journal of the American Society for Horticultural Science* **126,** 195–199.

López-Sáez JF, Gimenez-Martin G, González-Fernández A. 1966. Duration of cell division cycle and its dependence on temperature. *Zeitschrift für Zellforschung* **75,** 591–600.

Matsumura T. 2000. Cellular genealogy of *in vitro* senescence and immortalization. In: Macieira-Coelho A, ed. *Cell immortalization*. Berlin: Springer-Verlag, 103–119.

Melaragno JE, Mehrotra B, Coleman AW. 1993. Relationship between endopolyploidy and cell size in epidermal tissue of *Arabidopsis*. *The Plant Cell* **5,** 1661–1668.

Nagl W. 1976. DNA endoreduplication and polyteny understood as evolutionary strategies. *Nature* **261,** 614–645.

Schweizer L, Yerk-Davis GL, Phillips RL, Srienc F, Jones RJ. 1995. Dynamic of maize endosperm development and DNA endoreduplication. *Proceedings of the National Academy of Sciences, USA* **92,** 7070–7074.

Smulders MJM, Rus-Kortekaas W, Gilissen LJW. 1995. Natural variation in patterns of polysomaty among individual tomato plants and their regenerated progeny. *Plant Science* **106,** 129–139.

Sugimoto-Shirasu K, Roberts K. 2003. 'Big it up': endoreduplication and cell-size control in plants. *Current Opinion in Plant Biology* **6,** 544–553.

Traas J, Hülskamp M, Gendreau E, Höfte H. 1998. Endoreduplication and development: rule without dividing? *Current Opinion in Plant Biology* **1,** 498–503.

Webster PL, MacLeod RD. 1980. Characteristics of root apical meristem cell population kinetics: a review of analyses and concepts. *Environmental and Experimental Botany* **20,** 335–358.

Weinl C, Marquardt S, Kuijt SJH, Nowack MK, Jakoby MJ, Hülskamp M, Schnittger A. 2005. Novel functions of plant cyclin-dependent kinase inhibitors, ICK1/KRP1, can act non-cell-autonomously and inhibit entry into mitosis. *The Plant Cell* **17,** 1704–1722.

Yang L, Han Z, MacLellan WR, Weiss JN, Qu Z. 2006. Linking cell division to cell growth in a spatiotemporal model of the cell cycle. *Journal of Theoretical Biology* **241,** 120–133.